View metadata, citation and similar papers at core.ac.uk

brought to you by CORE

provided by Elsevier - Publisher Connector

BioSystems 146 (2016) 91–101

BioSystems

journal homepage: www.elsevier.com/locate/biosystems

Multi-objective shadow prices point at principles of metabolic regulation

Max Sajitz-Hermstein*, Zoran Nikoloski

Systems Biology and Mathematical Modeling Group, Max Planck Institute of Molecular Plant Physiology, Am Mühlenberg 1, 14476 Potsdam, Germany

ARTICLE INFO

Article history:
Received 26 January 2016
Accepted 4 April 2016
Available online 14 June 2016

ABSTRACT

Perturbations in environmental and intracellular conditions often lead to changes across all cellular layers, from transcription to metabolism. Regulatory mechanisms are key to mediating these changes to maintain homeostasis and to ensure viability. Since changes in metabolic reaction rates are partly due to perturbations in metabolite concentrations, it is expected that metabolites with large effect on those reaction rates which govern metabolic functionality are tightly regulated. The extent of metabolic regulation has been quantified by the sensitivity of an individual metabolic function to changes in metabolite concentrations, in particular by shadow prices in the constraint-based modeling framework. However, the system-wide characterization of the extent to which metabolite concentrations are regulated in the more realistic scenario of multiple contending tasks remains elusive. Here we examine multi-objective shadow prices for the central carbon metabolism of *Escherichia coli* whose reaction rates are shaped by several contending metabolic functions. We determine shadow prices for sampled solutions of the Pareto front, which characterizes the space of multi-objective optima, for three contending metabolic functions that provide the best agreement with ^{13}C-labeling experiments. By analyzing the parts of the Pareto front closest to the experimentally determined flux phenotypes, we show that *E. coli* operates in the vicinity of an area of the Pareto front which facilitates robust and efficient regulation. In addition, we find significant associations between features of the transcriptional regulatory network and the sensitivity of *E. coli*'s metabolic functionality to changes in metabolite concentrations. We demonstrate that the structural constraints of the metabolic network together with data on condition-specific flux phenotypes can be effectively used to dissect metabolic regulation on a system-wide level.

© 2016 The Author(s). Published by Elsevier Ireland Ltd. This is an open access article under the CC BY-NC-ND license (http://creativecommons.org/licenses/by-nc-nd/4.0/).

1. Introduction

Biological systems perpetually sense and respond to changes in environmental and intracellular conditions Kitano (2007). To ensure continuous functionality, maintain homeostasis, and to guarantee proliferation, cellular systems usually adapt to the perceived changes via an integrated response of their cellular networks. The system-wide response is ultimately reflected in the flux phenotype and levels of components (*e.g.*, transcripts, proteins, metabolites). The flux phenotype, which determines metabolic functionality, is characterized by the rates of the biochemical reactions in the underlying metabolic network and directly depends on the concentration of metabolites as well as the concentration and activity of enzymes. To ensure homeostasis on the level of fluxes, concentrations of metabolites with large effect on the flux phenotype are expected to be tightly regulated Fell (2005).

The molecular mechanisms by which metabolic regulation is exerted differ in timescale. A change of the metabolic state, *i.e.*, reaction fluxes and metabolite concentrations, is largely achieved by transcriptional regulation and takes place on the scale of minutes to hours Desvergne et al. (2006). In contrast, mechanisms relevant for correcting imbalances on shorter timescales are likely to involve post-translational modifications Helm (2006) and allosteric regulation Chubukov et al. (2014). Experimental *in vivo* study of the effects of allosteric regulation on the systems level is inherently difficult Motlagh et al. (2014), as it requires the arduous targeted manipulation of individual metabolite concentrations. An indirect way to learn about these short-term regulatory events, which aim at mitigating the effect of concentration fluctuations on the flux phenotype, is to determine how they relate to the topology of the underlying metabolic network.

To this end, shadow prices represent one means to derive and examine organization principles of metabolic regulation by

* Corresponding author. Tel.: +49 3315678622.
E-mail address: sajitz@mpimp-golm.mpg.de (M. Sajitz-Hermstein).

http://dx.doi.org/10.1016/j.biosystems.2016.04.005
0303-2647/© 2016 The Author(s). Published by Elsevier Ireland Ltd. This is an open access article under the CC BY-NC-ND license (http://creativecommons.org/licenses/by-nc-nd/4.0/).

employing the structure of the metabolic network. Shadow prices describe the sensitivity of the objective function of a linear program upon perturbation of individual constraints Bazaraa et al. (2010). In a cellular setting, shadow prices have been employed to analyze the change of the optimal flux phenotype upon imbalance of a given metabolite's concentration (*i.e.*, due to its accumulation or depletion) in the framework of flux balance analysis Varma and Palsson (1994), Savinell et al. (1992), Savinell and Palsson (1992). Specifically, shadow prices quantify the change in a metabolic objective (*e.g.*, maximization of biomass yield) upon increase/decrease in metabolic flux of individual reactions leading to a deviation from steady state.

It has recently been shown that shadow prices are suitable predictors of temporal variation of individual metabolite concentrations as well as indicators of their growth-limiting effects Reznik et al. (2013). As a result, shadow prices can be used to examine the requirement for regulating individual metabolite concentrations solely based on a stoichiometric model of the metabolic network and an assumed metabolic objective. If the absolute value of a shadow price is large, perturbations of the corresponding metabolite concentrations are expected to have large effect on metabolic function and should, therefore, be tightly regulated (*e.g.*, by high concentrations of the synthesizing and degrading enzymes).

The existing studies have concentrated only on shadow prices for a single objective function. However, it was shown that using a combination of multiple objective functions leads to higher accuracy of the predicted flux phenotypes Schuetz et al. (2007). For the case of *Escherichia coli*, a multi-objective analysis established that flux phenotypes determined under different environmental conditions could be best described by combining two efficiency objectives (maximization of biomass yield, maximization of ATP yield) and one optimal resource allocation objective (minimization of total flux) Schuetz et al. (2012). Moreover, it was found that flux phenotypes are in a close vicinity to the Pareto front describing the set of non-inferior solutions, i.e., flux phenotypes which can only improve one objective at the expense of reducing at least one other.

Here, following the work of Schuetz et al. (2012), we examine shadow prices with respect to multiple contending objectives in the central carbon metabolism of *E. coli* to obtain insights in metabolic regulation and its relation to the structure of the metabolic network. For representative solutions of the Pareto front, shadow prices of metabolites are determined individually for each of the three objective functions which were found to provide best agreement between experimentally determined and predicted flux distributions. By using ^{13}C flux estimates for non-limited as well as carbon- and nitrogen-limited aerobic conditions, we investigate shadow prices in the physiologically relevant section of the Pareto front in which the cell operates under these conditions.

2. Results

We examine sensitivity of the flux phenotype with respect to changes of metabolite concentrations in the multiple-objective scenario for the model of *E. coli*'s central carbon metabolism developed by Schuetz et al. (2007) (see Fig. S1 and Tables S1 & S2). A multi-objective optimization problem usually has no unique solution due to the trade-off between individual objectives. Here, we focus on Pareto-optimal solutions, *i.e.*, solutions which cannot be improved with respect to an individual objective without deteriorating the optimal achievable value of at least one of the other objectives. The entirety of such solutions forms the Pareto front. Each Pareto-optimal solution is associated with a set of shadow prices for every objective and each metabolite.

Here, we determine a representative set of the Pareto front solutions (for brevity, in the following we refer to the representative set as the Pareto front) emerging from three contending objectives: (i), maximizing biomass yield, (ii), maximizing ATP yield, and (iii), minimizing total flux. Schuetz et al. showed that these objectives yield flux phenotype predictions closest to *in vivo* ^{13}C flux estimates in the central carbon metabolism of *E. coli* for a range of environmental conditions Schuetz et al. (2012). The Pareto front together with the projection of the polyhedral cone of steady-state flux distributions on the three contending objectives alongside the experimentally determined flux distributions is shown in Fig. 1. Schuetz et al. demonstrated that, for the examined environments, *E. coli* exhibited flux phenotypes which were located in close

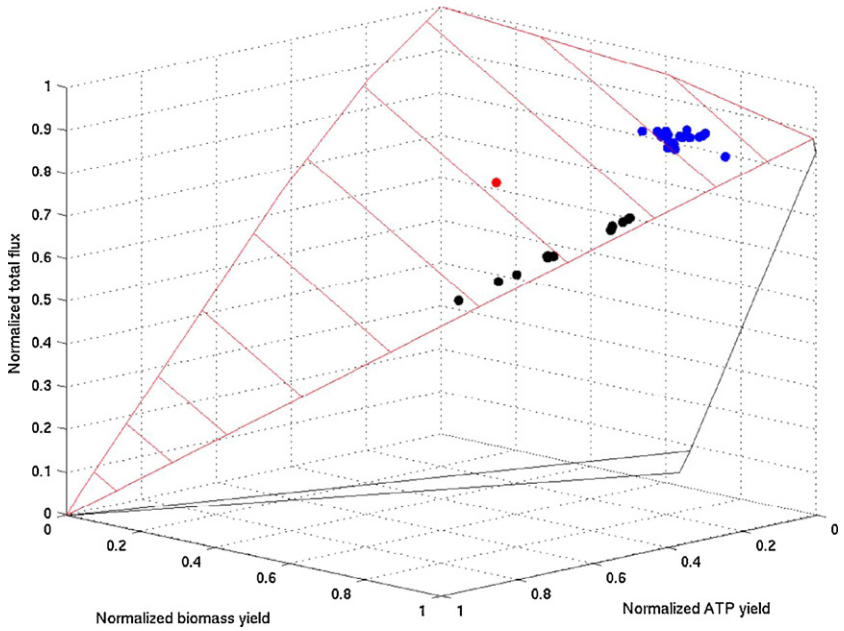

Fig. 1. Visualization of the Pareto front. The flux cone (solution space of flux balance analysis) is obtained via elementary flux mode analysis and is projected onto the three contending metabolic objectives. The Pareto front is highlighted in red. Parts of the flux cone corresponding to minimum total flux larger than the minimum observed for zero ATP and zero biomass yield are excluded. Experimentally determined flux distributions (aerobic conditions) are shown as dots: non-limited (blue), carbon-limited (black), nitrogen-limited (red).

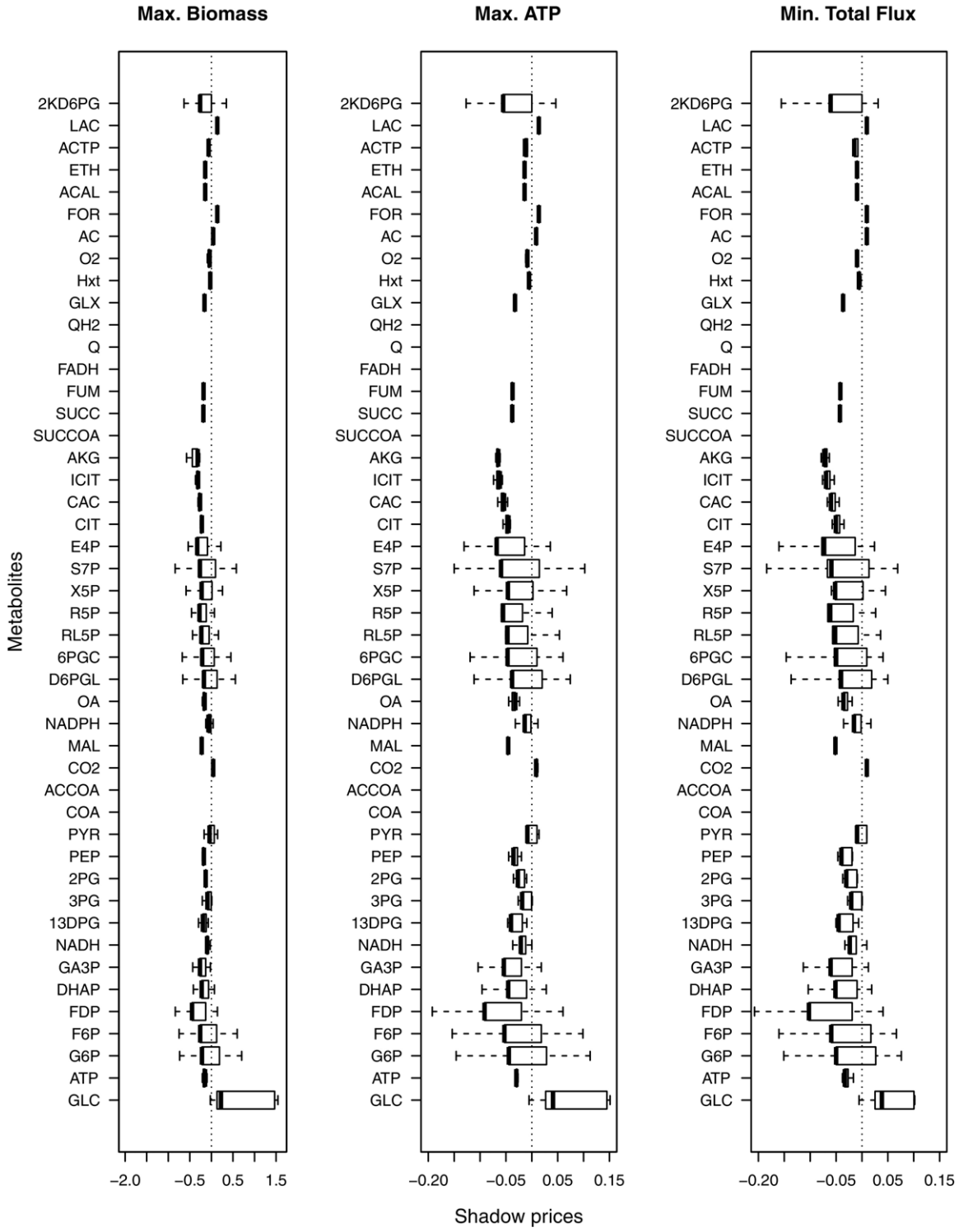

Fig. 2. Boxplots of shadow price distributions. The shadow price distributions are obtained utilizing the set of sampled optimal flux distributions representing the Pareto front. To enable better comparison of distributions, the *x*-axis is scaled up by a factor 10 in the cases of maximization of ATP yield and minimization of total flux.

vicinity to the Pareto front Schuetz et al. (2012). To obtain insights into the adaptation of regulatory mechanisms employed as a result of environmental shifts, we examine the sensitivity of these experimentally determined flux phenotypes, which were obtained under non-limited as well as under carbon- and nitrogen-limited aerobic conditions.

The utilization of shadow prices as a measure of sensitivity with respect to individual Pareto-optimal solutions is hindered in two cases. The first case is characterized by the occurrence of two-sided (ambiguous) shadow prices, *i.e.*, shadow prices depending on the direction of perturbation, which is the result of degeneracy of the linear program Strum (1969). This is particularly relevant with respect to fluctuations of metabolite concentrations, which are perturbations of the steady state in both directions (*i.e.*, due to depletion and accumulation of a metabolite). Two-sided shadow prices are then an indicator of instability, because they are expected to lead to a continuously growing effect of the direction exhibiting larger sensitivity. The second case is characterized

by infeasibility of the optimization problem in which the steady-state constraint for a given metabolite is perturbed. This means high fragility of metabolic functionality with respect to concentration fluctuations of the metabolite. In both cases we cannot quantify sensitivity uniquely, but each is an indicator of large sensitivity. To avoid issues of ambiguity and infeasibility, we restrict our quantitative analysis to true shadow prices, *i.e.*, shadow prices which do not depend on the direction of perturbation. In the following, we analyze the distribution of shadow prices across the Pareto front as well as among the Pareto-optimal solutions closest to physiological flux phenotypes.

Table 1
Mean/median shadow prices of contending objectives are highly correlated. Means/medians of shadow prices with respect to the objectives maximization of biomass yield (BM), maximization of ATP yield (ATP) and minimization of total flux ($\sum_i |f_i|$) are calculated across the whole Pareto front; association is determined via Kendall's rank correlation coefficient.

	Mean	Median
BM vs. ATP	0.88*	0.97*
BM vs. $\sum_i \lvert f_i \rvert$	0.75*	0.95*
ATP vs. $\sum_i \lvert f_i \rvert$	0.97*	0.99*

* indicates significant association, $P < 10^{-5}$.

2.1. Phenotype dependency of sensitivity

The Pareto front comprises the entirety of optimal flux phenotypes with respect to the three objectives, and can be regarded as a characterization of the range of potential metabolic behavior. The shadow prices for the majority of metabolites vary across the Pareto front (see Fig. 2), whereby biomass yield exhibits distinctly larger values compared to the other objectives. This implies that the sensitivity of metabolic functionality towards fluctuations of metabolite concentrations depends on the particular flux phenotype. The distributions of shadow prices for the three objectives are very similar (Fig. 2), which is corroborated by the association of the mean/median values for each pair of objectives over the whole Pareto front (Table 1). We further investigate on the similarity of shadow price distributions in Section 2.2.

A change of the flux phenotype is triggered by external or internal cues and reflects the alteration of the interplay between

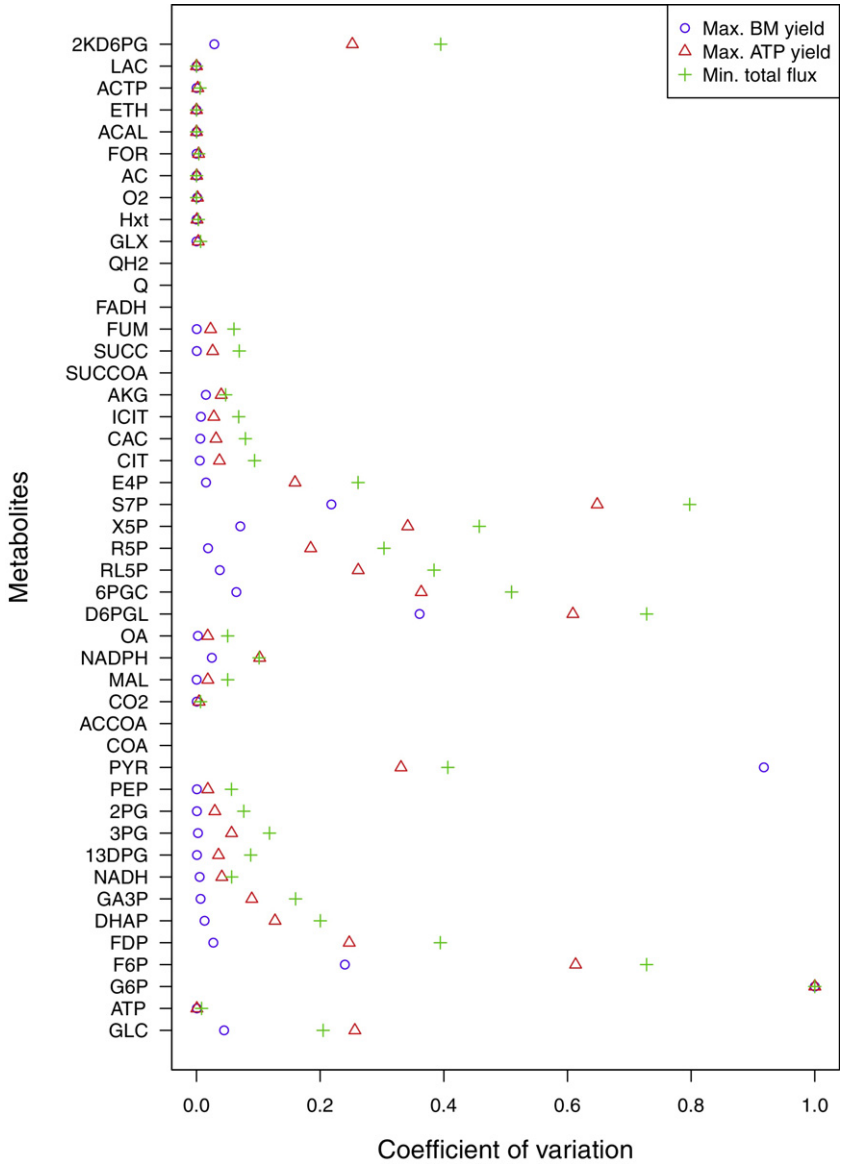

Fig. 3. Normalized coefficients of variation. Similar patterns are observed for all three objectives.

particular metabolic pathways. Such change can be associated with a movement across the Pareto front. The accompanying variation of sensitivity is likely to be pathway dependent, which would imply that metabolites involved in a particular pathway are similarly regulated. To compare the variation of sensitivity of individual metabolites, we calculate the normalized coefficient of variation

$$\hat{CV}_i^{\text{obj}} = \frac{CV_i^{\text{obj}}}{\max_i CV_i^{\text{obj}}}, \text{ with}$$

$$CV_i^{\text{obj}} = \frac{\sigma_i^{\text{obj}}}{|\mu_i^{\text{obj}}|},$$

whereby σ_i^{obj} and μ_i^{obj} denote the standard deviation and mean of shadow prices of metabolite i across the whole Pareto front with respect to an individual metabolic objective. We utilize the absolute value of the mean to guarantee a positive value. Indeed, we find largest variation of sensitivity for metabolites involved in particular pathways, namely glycolysis, the pentose phosphate pathway and the Entner–Douderoff pathway (Fig. 3). While the observed behavior is similar for all three objectives, larger coefficients of variation are found for the maximization of ATP yield and the minimization of total flux.

Examining the cases which do not exhibit true shadow prices suggests that the central carbon metabolism of *E. coli* is very sensitive to fluctuations in cofactor levels for all phenotypes. We find no true shadow prices with respect to all three objectives for several cofactors, namely, CoA, acetyl-CoA, succinyl-CoA, FADH, ubiquinol and ubiquinone. This is in line with their role for cell vitality – without these cofactors the TCA cycle and most of the fermentation pathways cannot proceed and ATP production would be limited to glycolysis. Therefore, it is expected that the levels of these metabolites are tightly regulated. The cofactors ATP, NADH and NADPH exhibit true shadow prices in most cases; however, the reason may be the boundary of the utilized metabolic network model, in which the metabolites replenishing these cofactors (ADP, NAD and NADP) do not have to obey the steady-state condition.

Our results indicate that *E. coli* operates near parts of the Pareto front exhibiting true shadow prices for most of the metabolites, implying that realization of flux phenotypes is rarely accompanied by extremely large sensitivity. We find true shadow prices for most of the non-cofactor metabolites across the entire Pareto front. However, in cases where substantial areas of the Pareto front do not exhibit true shadow prices, the majority does exhibit true shadow prices for the physiologically realized flux phenotypes (see Table 2). It should be noted that single-objective shadow price analysis utilizing minimization of total flux does not result in true shadow prices for most metabolites (see Fig. S2), which leads to the presumably erroneous conclusion of extremely large sensitivity. We observe that glucose, formate, acetaldehyde, lactate and ethanol do not exhibit true shadow prices for a large area of the Pareto front, including the Pareto optimal solutions pertaining to experimentally observed fluxes. This is in agreement with the fact that these four metabolites are potential substrates for *E. coli*, for which reason their levels are expected to be highly regulated.

Table 3
Shadow prices of physiological flux phenotypes are significantly associated with static features of the transcriptional network. Association is determined via Kendall's rank correlation coefficient, between the mean shadow prices across the whole Pareto front and across measured ^{13}C flux distributions, respectively, and the total number of transcription factors acting on reactions involving the individual metabolites.

	Whole Pareto front	p-value	^{13}C fluxes	p-value
Max. biomass	−0.20	0.08	−0.32	0.01
Max. ATP production	−0.15	0.19	−0.33	0.01
Min. total flux	−0.14	0.21	−0.33	0.01

Intriguingly, some metabolites exhibit positive shadow prices (Fig. 2), which implies an unexpected behavior. For instance, in the case of maximization of biomass yield, a positive shadow price for a metabolite indicates that biomass yield decreases if an additional amount of the metabolite is introduced. This can be explained by the interplay of multiple objectives, namely from the minimization of total flux which drives the system to reroute flux upon imbalance in the metabolite, which can lead to a lower biomass yield. In the following, we examine only absolute values of shadow prices, since positive shadow prices are equally an indicator of the sensitivity of metabolic functionality upon concentration changes.

2.2. *Efficiency of regulatory mechanisms in* Escherichia coli

For every Pareto-optimal solution and every metabolite we calculate three shadow prices, one for each objective, often resulting in three different values. The regulatory action on an individual metabolite concentration is expected to meet the regulatory demands arising from all of these sensitivities. When a change in the metabolic state occurs, it may be accompanied by an opposing change of sensitivities, *i.e.*, to an increased requirement for regulating a metabolite concentration with respect to one objective and a decreased requirement with respect to another. To enable robust

Table 2
Pareto front coverage with true shadow prices. Coverage for individual metabolites is given in per cent, only metabolites exhibiting less than 99% coverage are shown. Checkmarks indicate if true shadow prices are observed for all experimentally determined flux distributions.

	Max. biomass yield	Max. ATP yield	Min. total flux	Phys. fluxes covered
AC	80.6	82.1	82.1	√
ACTP	80.6	82.1	82.1	√
MAL	57.8	57.8	57.8	√
SUCC	57.8	57.8	57.8	√
FUM	57.8	57.8	57.8	√
GLX	57.6	57.6	57.6	√
GLC	21.3	20.1	21.3	×
FOR	12.0	11.9	12.2	×
LAC	11.3	11.5	11.7	×
ACAL	4.8	4.1	5.2	×
ETH	4.8	3.8	4.9	×
COA	0	0	0	×
ACCOA	0	0	0	×
SUCCOA	0	0	0	×
FADH	0	0	0	×
Q	0	0	0	×
QH2	0	0	0	×

and efficient regulation, it would be beneficial if the cell could meet the change in regulatory requirements with respect to all the objectives with as few regulatory mechanisms as possible. Opposing changes of shadow prices with respect to individual objectives upon shifts in environmental conditions would suggest that concurrent regulatory mechanisms have to be utilized. To determine whether or not sensitivities change concordantly, we examine the association of shadow prices between the individual objectives across the Pareto front.

Based on Kendall's rank correlation coefficient, we find for most of the metabolites that shadow prices across the whole Pareto front as well as across the experimentally determined flux phenotypes are positively correlated for each pair of the objectives (see Fig. 4). In comparison, correlations are overall considerably larger and more metabolites show large correlations in the case of the experimentally observed flux distributions. Most importantly, associations of shadow prices for the experimentally observed flux distributions are very stable across metabolites, in contrast to the whole Pareto front. This indicates that the central carbon metabolism of *E. coli* operates close to those parts of the Pareto front which facilitate adaptation to environmental changes with low requirement for concurrent mechanisms to regulate individual metabolite concentrations.

Opposing changes of shadow prices across the physiological flux distributions, indicated by anticorrelation, are observed in few cases, namely, acetate, carbon dioxide, glyceraldehyde 3-phosphate, oxygen and succinate. The concentrations of these metabolites are expected to be regulated by multiple mechanisms. Glyceraldehyde 3-phosphate, which is a biomass component as well as the central metabolite in the interplay between glycolysis, pentose phosphate pathway and the Entner–Douderoff-pathway, exhibits considerable anticorrelation ($\tau \approx -0.5$) for maximizing ATP and biomass yield. Opposing regulatory requirements seem reasonably given its large involvement in partially opposing metabolic functions. In the case of acetate and succinate, the observation is in line with the fact that both play important roles in the regulation of enzymes via acetylation and succinylation Gerosa and Sauer (2011), indicating the diversity of biologic processes affected by their levels. This diversity highly suggests a multiplicity of mechanisms to regulate these metabolite concentrations.

Another factor shaping regulatory requirements, besides the number of regulatory mechanisms needed, is the total variation of individual sensitivities. Each change of sensitivity should be accommodated by putting in place a regulatory mechanism (*e.g.*, by increasing the concentration of synthesizing and degrading enzymes). Since each such specific regulatory mechanism requires

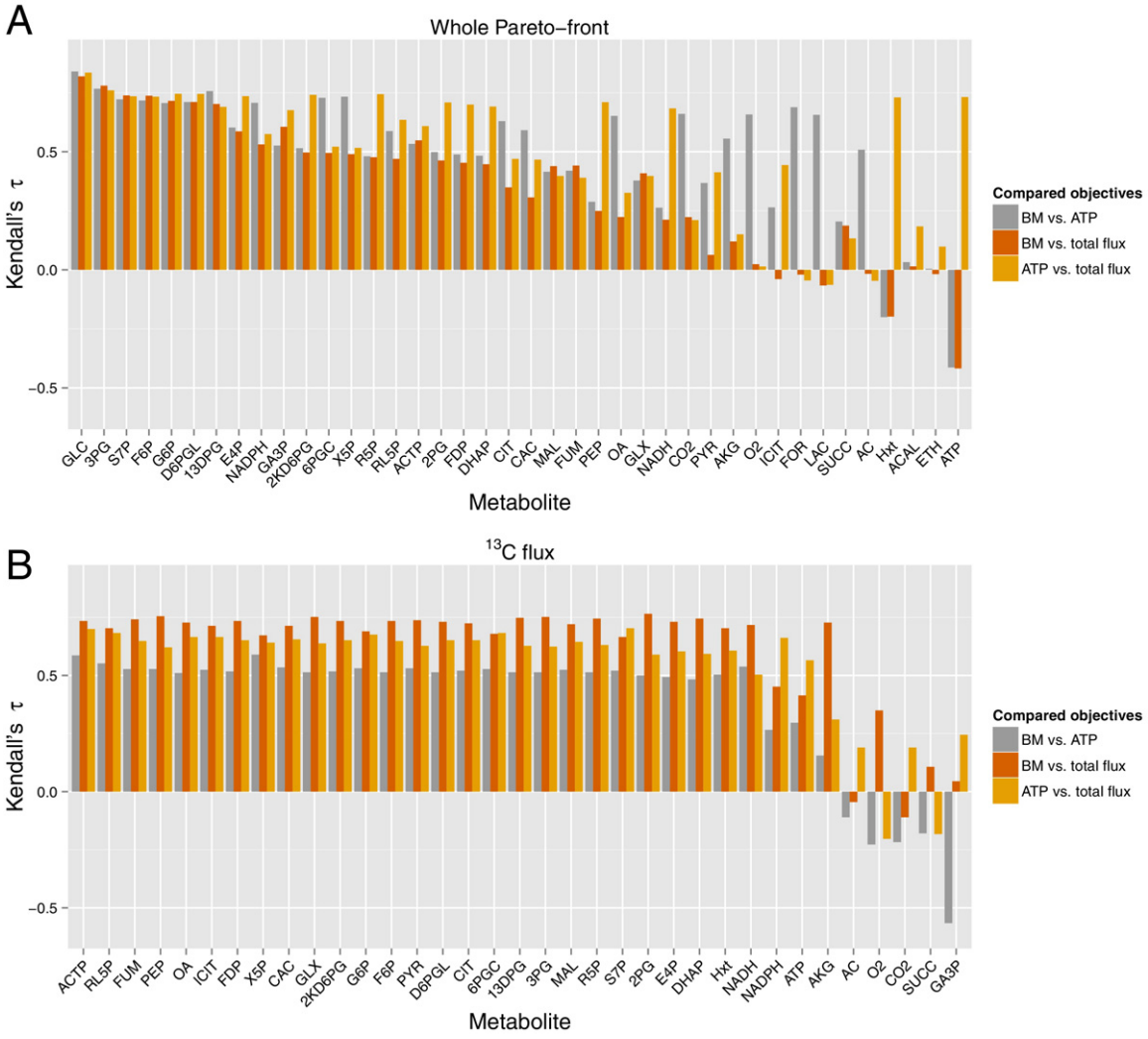

Fig. 4. Associations between shadow prices of contending objectives are higher and more stable in the case of physiological flux phenotypes. Associations are determined via Kendall's rank correlation coefficient for each two out of the three objectives considering: (A) the whole Pareto front, and (B) only the flux distributions obtained from ^{13}C measurements. Associations are shown in decreasing order with respect to the average of correlation coefficients across all pairs of objectives.

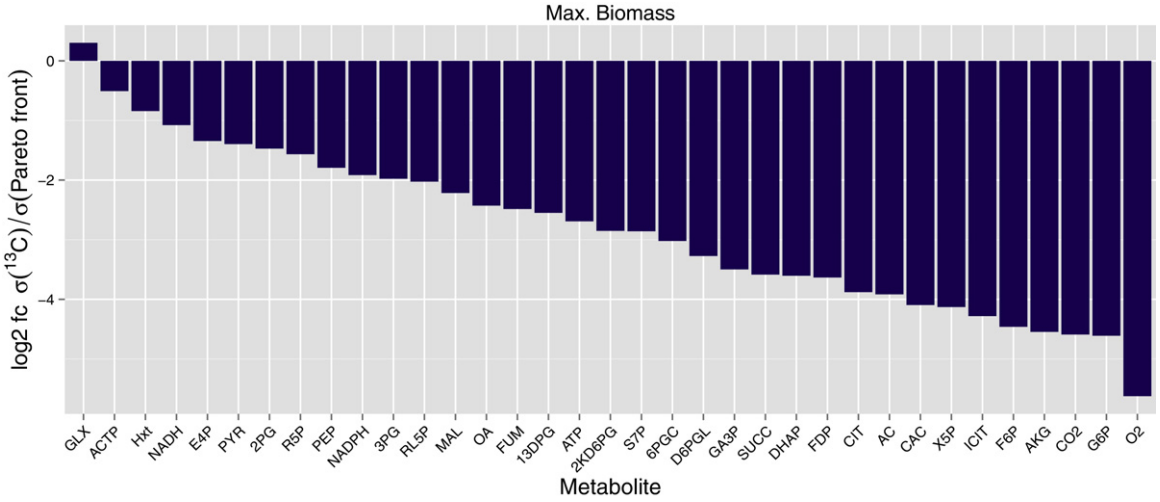

Fig. 5. Variability of shadow prices (max. biomass yield) decreases for physiological flux phenotypes compared to the admissible solution space. Change of variability is shown by the log2-fold ratio of the standard deviation of absolute shadow prices for the whole Pareto front and for the flux distributions obtained from ^{13}C measurements.

resources, one would expect that the changes in sensitivities are minimized for efficient and robust regulation. To test this hypothesis, we examine the variation of individual shadow price distributions. With respect to the objective of biomass yield maximization, we compare shadow price standard deviations for the whole Pareto front with the ones for the experimentally determined flux distributions (see Fig. 5). Except for glyoxylate, we observe a drastically reduced standard deviation for the experimentally determined flux distributions. This indicates a heavily attenuated need for adapting regulatory mechanisms within the physiologically realized flux phenotypes compared to the admissible optimal flux phenotypes.

2.3. The effect of environmental shifts on sensitivity

Environmental shifts affect the shadow prices of physiologically realized flux phenotypes, although the effect is reduced compared to the entire Pareto front. We find that all objectives exhibit larger shadow prices with respect to fluctuations of metabolites in the pentose phosphate pathway (PPP) under conditions of carbon- as well as nitrogen-limitation in comparison to non-limiting conditions (see Fig. 6 for the case of maximization of biomass yield switching from non- to carbon-limited conditions and Figs. S3–S7 for the other cases). In contrast, the shadow prices are reduced with respect to metabolites found in glycolysis and in the TCA cycle. These observations suggest that regulation of metabolite concentrations should be adapted towards tighter regulation in the case of the PPP and towards looser regulation in the case of glycolysis and the TCA cycle. When the environment becomes limiting, ATP yield increases with the decrease in biomass yield (see Fig. 1). Therefore, from an evolutionary viewpoint, the change of sensitivity might be the result of an adaptation of the metabolic network topology towards minimizing the regulatory requirement for metabolic pathways which are most important under specific conditions (*e.g.*, for glycolysis and the TCA cycle, which are central to high ATP yield, when switching from non-limiting to limited conditions). The same argument holds when switching from limited to non-limiting conditions for the predominantly anabolic PPP which is very important for biomass production.

2.4. Sensitivity and static features of metabolic regulation

Currently, there exists no experimental approach which would allow the direct validation of the relationship between shadow

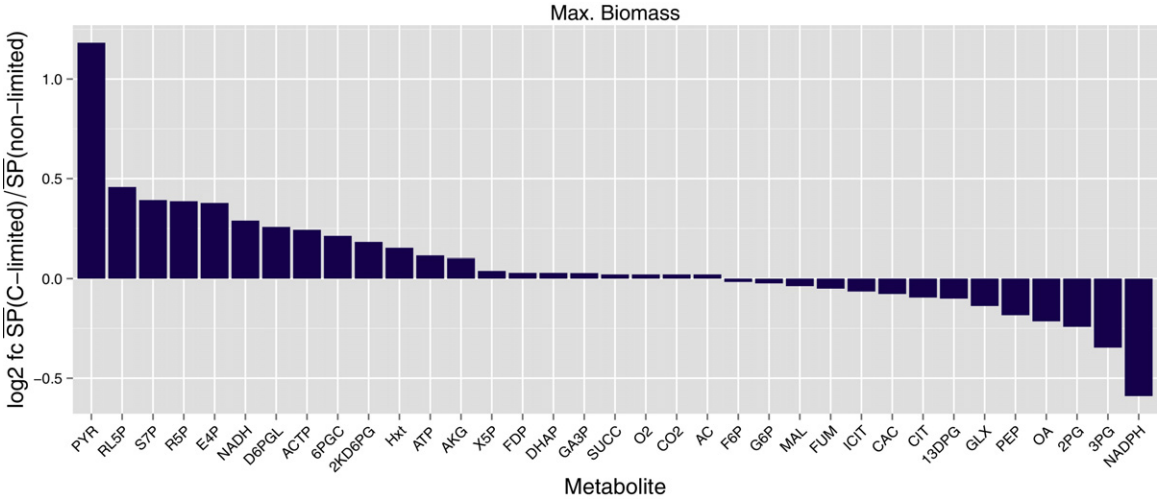

Fig. 6. Shadow prices (max. biomass yield) change as a result of the shift from non-limited to carbon limited conditions. The change of shadow prices is shown by the log2-fold ratio of the means of absolute shadow prices pertaining to the physiologically observed flux distributions under non- and carbon-limited aerobic conditions.

prices and the regulation of metabolite concentration fluctuations. Although fluctuations of metabolite concentrations cannot be assessed, we can test if there exists a relationship with respect to transcriptional regulation. To this end, we examine the association of shadow prices with static features of transcriptional regulation, which accounts for movements on the Pareto-front. To this end, we examine the correlation between the total number of transcription factors acting on reactions involving a particular metabolite and the mean shadow prices across the whole Pareto front as well as across measured ^{13}C flux distributions, respectively. The number of transcription factors is taken from the RegulonDB database Salgado et al. (2013). Negative correlation indicates that the more an objective is sensitive upon fluctuation of a metabolite concentration, the fewer transcription factors are involved in regulating the reactions which directly utilize the metabolite. This would imply that regulation of concentrations of metabolites, which are growth-limiting under the examined conditions, is exerted by only few transcription factors. Indeed, we find significant negative correlations in case of the physiological flux phenotypes with respect to all objectives (see Table 3). This result corresponds to our finding that *E. coli* realizes flux phenotypes which allow regulation of individual metabolite concentrations with a minimum of concurrent regulatory mechanisms. Therefore, the tight regulation of metabolite concentrations due to the higher growth-limiting effect of individual metabolites is met by a smaller number of transcriptional regulatory factors compared to the less limiting metabolites. Importantly, we do not find a significant association utilizing the mean of shadow prices across the whole Pareto front. Our findings indicate that *E. coli* has optimized the network topology as well as the realization of the flux phenotype such that growth-limiting metabolites can be effectively regulated with few regulatory mechanisms.

3. Discussion

Based only on static properties of metabolic networks, the analysis of multi-objective shadow prices allows predicting the sensitivity of flux phenotypes with respect to fluctuations in metabolite concentration and, therefore, facilitates insights in the accompanying regulatory requirements. Integration of such sensitivity analysis based on the natural assumption of multiple contending metabolic functions governing the flux phenotype with ^{13}C flux data allows to compare the properties of theoretically admissible optimal flux phenotypes with the physiologically realized ones. Moreover, it enables the investigation of trade-offs between multiple cellular objectives, how they relate to the regulatory requirements, and how these requirements may differ between environmental conditions.

We found several indicators of evolutionary adaption with respect to the regulation of metabolism in the central carbon metabolism in *E. coli*. Our findings indicate that *E. coli* operates near parts of the Pareto front exhibiting low requirement for concurrent mechanisms to regulate metabolite concentration fluctuations, allowing efficient and robust regulation. The requirement for adjusting the strength of regulation appears drastically reduced for experimentally observed flux phenotypes in comparison to the theoretically admissible ones. Nevertheless, metabolites within pathways which are important to ensure viability under limiting conditions showed reduced sensitivity, which hints at an optimization of network topology to stabilize metabolic function with respect to metabolite concentration fluctuations. Most strikingly, we found an association between the regulatory requirements, arising solely from the topology of the metabolic network, with static features of the transcriptional regulatory network. The observed correlations are high considering that we take into account only static features of metabolic regulation at the level of transcription, neglecting dynamic as well as post-translational effects. Our observations hint at the mutual influence during the development of the topologies of these networks.

The insights generated by multi-objective shadow prices can help to further elucidate the interactions of metabolite concentrations, reaction fluxes and the variety of regulatory events on the systems level. A better understanding of these key determinants of cellular state will have direct implications for metabolic engineering as well as pharmaceutical treatments. In the latter, multi-objective shadow price analysis may facilitate screening for targets of regulatory mechanisms which are robust across condition-specific physiological phenotypes.

4. Materials and methods

4.1. Structural modeling

Structural (constraint-based) modeling examines the solution space of feasible flux distributions $\mathbf{f} \in \mathbb{R}^n$ across the n biochemical reactions of a metabolic network assuming that it operates at a (quasi) steady-state, *i.e.*, the concentrations $\mathbf{x} \in \mathbb{R}^m$ of the m metabolites in the network are constant. The steady-state condition can be written as $(\mathrm{d}/\mathrm{d}t)\mathbf{x} = S \cdot \mathbf{f} = \mathbf{b}$, whereby $\mathbf{b}$ is equal to zero for all internal metabolites, *i.e.*, metabolites obeying the steady-state condition; the stoichiometry matrix $\mathbf{S} \in \mathbb{R}^{m \times n}$ captures the individual reaction stoichiometries. External metabolites represent the connection to the environment and are allowed to violate the steady-state condition to establish import or export flux. The corresponding elements of $\mathbf{b}$ can then take values other than zero. Upper and lower boundaries of the flux vector $\mathbf{f}_{min} \leq \mathbf{f} \leq \mathbf{f}_{max}$ further constrain the solution space and can be used to realize physiologic properties like limitation of nutrient import and reaction reversibility, as well as environmental conditions.

4.2. Flux balance analysis

The steady-state condition and the flux boundaries determine the solution space which usually contains infinitely many flux distributions. To obtain a representative flux distribution as well as to probe the synthesizing capabilities of the network, flux balance analysis Varma and Palsson (1994), Orth et al. (2010) assumes that metabolic behavior is guided by some optimization principles, *e.g.*, optimization of resource utilization. If such an objective as well as the constraints of the solution space are linear, the optimization problem can be written as a linear program

$$\begin{aligned} \max_{\mathbf{f}} z = \sum_i c_i v_i, \quad i = 1, 2, \ldots, n, \text{ s.t.,} \\ \mathbf{S} \cdot \mathbf{f} = \mathbf{b} \\ \mathbf{f}_{\min} \leq \mathbf{f} \leq \mathbf{f}_{\max}. \end{aligned} \tag{1}$$

For example, a common choice for the objective function is the flux through a biomass reaction. The maximization of this objective function can be used to determine the theoretical maximum of biomass yield under specific conditions. Its application resulted in a wide range of predictions consistent with experimental observations for simple model organisms Edwards and Palsson (2000), Edwards et al. (2001), Ibarra et al. (2002). Other examples are minimization of ATP production which can be used to determine the conditions for energy efficiency, and minimization of nutrient uptake, which can be applied in modeling the case of nutrient scarcity (an overview of objective functions is provided by Schuetz et al. (2007)).

We denote the space of feasible solutions by Γ, here $\Gamma = \{\mathbf{f} \in \mathbb{R}^N | \mathbf{S} \cdot \mathbf{f} = \mathbf{b}, \mathbf{f}_{\min} \leq \mathbf{f} \leq \mathbf{f}_{\max}\}$.

Objective functions In accordance with Schuetz et al. (2012), we utilize three is objective functions: (i), maximizing biomass

yield, (ii), maximizing ATP yield and, (iii), minimizing total flux. These objective functions were shown to provide best predictions of *in vivo* fluxes determined by ^{13}C measurements Schuetz et al. (2012). Minimization of total flux $\min\sum_i|f_i|$ is executed via introduction of slack variables acting as boundaries on the original variables. For each reaction i a slack variable f_i' is introduced which enters the optimization problem in the form of additional constraints. Minimization of total flux can then be formulated as a linear program

$$\begin{aligned} \max_{\mathbf{f}'}(-1)\cdot\sum_i f_i', \text{ s.t.,}\\ \mathbf{S}\cdot\mathbf{f}=\mathbf{b}\\ \mathbf{f}_{\min}\le\mathbf{f}\le\mathbf{f}_{\max},\\ f_i\le f_i'\\ f_i\ge -f_i'\\ f_i'\ge 0. \end{aligned} \tag{2}$$

Solving this optimization problem is equivalent to solving the minimization problem $\min_{\mathbf{f}}\sum_i f_i'$. However, the sign of shadow prices changes with respect to formulation, although the interpretation does not change. Therefore, to simplify comparison between shadow prices calculated for different objectives, we use formulation (2). In the following, we denote by $\mathbf{f}$ the original flux vector plus slack variables.

4.3. Multi-objective optimization

Flux balance analysis crucially depends on the choice of an appropriate objective function, which may depend on environmental conditions and the cellular state. It is reasonable to assume that indeed multiple cellular objectives govern metabolism and that the individual objectives may be contending.

In the multi-objective case, due to the contending character of the individual objectives, a solution can usually only be found by weighting the individual contributions. The solution of such a weighted problem then represents a specific trade-off of cellular objectives.

Schuetz et al. examined the effect of multiple contending objectives on flux distributions, which enabled insight into the plasticity of metabolic behavior Schuetz et al. (2012). By replicating their analysis, we determine the Pareto front of the central carbon metabolism of *E. coli* for the three objective functions described in Section 4.2. We utilize shadow prices as a measure of sensitivity to analyze the influence of metabolite concentration fluctuations.

Pareto front A feasible solution $\mathbf{f}^*\in\Gamma$ to a multi-objective optimization problem (without loss of generality we consider maximization) with t objective functions z_i is called weakly Pareto-optimal if there does not exist another solution $\mathbf{f}\in\Gamma$ with $z_i(\mathbf{f})>z_i(\mathbf{f}^*)$ for all $i\in 1,\ldots,t$; it is called (strongly) Pareto-optimal if there does not exist another solution $\mathbf{f}\in\Gamma$ with $z_i(\mathbf{f})\ge z_i(\mathbf{f}^*)$ for all $i\in 1,\ldots,t$ and at least one j with $z_j(\mathbf{f})>z_j(\mathbf{f}^*)$. The Pareto front Γ^* of a multi-objective optimization problem (also called the set of non-inferior solutions) is given by the set of all (strongly) Pareto-optimal solutions.

While a parameterization of the Pareto front can be difficult, a set representing the Pareto front, the representative Pareto front, can be determined by the ε-constraint method, which successively samples solutions such that the entire Pareto front is covered.

ε-constraint method We determine a representative Pareto front via the ε-constraint method Miettinen (1999), which we describe (without loss of generality) for the case of maximization. To this end, one objective function $z_p=\sum_i c_i^{(p)}f_i$ is selected to be optimized while the remaining objective functions $z_q=\sum_i c_i^{(q)}f_i$ are converted into constraints with lower bounds ε_q. The ε_q are chosen from intervals defined by the minimum and maximum outcomes of the individual single-objective linear programs, $\varepsilon_q\in[\min z_q, \max z_q]$. The lower bounds are successively varied in k equidistant steps starting from the smallest value and the resulting (single-objective) linear programs are solved, such that all combinations of ε_q are visited (we choose $k=100$). The optimization problem can be formulated as

$$\begin{aligned} \max_{\mathbf{f}} z_p=\sum_i c_i^{(p)}f_i, \text{ s.t.}\\ \mathbf{S}\cdot\mathbf{f}=\mathbf{b},\\ \mathbf{f}_{\min}\le\mathbf{f}\le\mathbf{f}_{\max},\\ z_q=\sum_i c_i^{(q)}f_i\ge\varepsilon_q\quad \forall q\in 1,\ldots,o\neq p, \end{aligned} \tag{3}$$

whereby o denotes the number of objectives. Each feasible solution gives a weakly Pareto-optimal solution of the multi-objective problem Miettinen (1999), *i.e.*, other objectives could still improve. To obtain a (strongly) Pareto-optimal solution (and, therefore, an element of the Pareto front), the optimal outcome z_p^* of Eq. (3) is added as a constraint $z_p=z_p^*$ to the constraint set of Eq. (3). A linear program with this constraint set which optimizes one of the other objective functions is solved and the outcome is added again as an additional constraint. This is repeated until all objective functions were tested, the final solution is then guaranteed to be (strongly) Pareto-optimal Miettinen (1999). It should be noted, that a parameterization would be needed to determine a truly unbiased sampling of Pareto-optimal solutions. However, since the Pareto surface in our case is very flat (see Fig. 1) and we determine minimum flux for fixed biomass and ATP production which are varied in equidistant steps, the introduced bias is non-qualitative and negligible.

4.4. Shadow prices

Shadow prices quantify the effect of perturbing the optimization problem's constraints on the optimization outcome. For illustration, without loss of generality, let's assume we have an equality constraint. Any equality constraint on a vector $\mathbf{f}$ can be written in the form $c_i(\mathbf{f})=b_i$. In the case of a single objective function z, the shadow price with respect to the i-th constraint is denoted by $(\partial z/\partial b_i)$. It quantifies the change of the optimal outcome of the objective function if the i-th constraint is perturbed. Here, it can be interpreted as the effect of perturbing the steady-state with respect to individual metabolite concentrations, in particular the sensitivity of an optimal objective function outcome, like maximum biomass yield, on concentration fluctuations. A more detailed consideration of shadow prices with respect to flux balance analysis is provided by Reznik et al. (2013).

It should be noted that linear programming solvers usually provide the values of the dual variables at an optimal solution, which coincide with the shadow prices if the solution is not degenerate. If a solution is degenerate, which is not uncommon, the values of the dual variables do not have to coincide with the shadow prices. Therefore, we refrain from using the dual variables and, instead, calculate shadow prices by two additional linear programs determining the decremental and incremental shadow price Ho (2000), Reznik et al. (2013). In the case of degenerate solutions, two-sided shadow prices may be found, *i.e.*, shadow prices with values depending on the sign of perturbation. To prevent uncertainties arising from two-sided shadow prices, we restrict our analysis to true, *i.e.* not two-sided, shadow prices.

In the multi-objective case, we calculate shadow prices individually for each objective function and each solution of the representative Pareto front. To this end, we fix all but one of the objective

functions to the values of the chosen Pareto-optimal solution, and calculate the effects of perturbing the steady-state constraints (corresponding to the individual metabolites) on the remaining objective. Our approach is similar to the one of McCarl et al. who decompose multiple objective shadow prices into shadow prices with respect to the individual objectives McCarl et al. (1996).

To calculate decremental and incremental shadow prices with respect to an individual metabolite w and objective function p in the multi-objective setting two linear programs are solved, which can be written as

$$\begin{aligned} \max z_p^{\mathrm{de/in}} &= \sum_i c_i^{(p)} f_i, \text{ s.t.} \\ \mathbf{S}\cdot\mathbf{f} &= \mathbf{b}^*, \\ \mathbf{f}_{\min} \le \mathbf{f} &\le \mathbf{f}_{\max}, \end{aligned} \tag{4}$$

$$b_j^* = \begin{cases} b_j, & \text{if } j \neq w \\ b_j \mp \pi_w^{\mathrm{de/in}}, & \text{if } j = w. \end{cases}$$

We perturb the equality constraint pertaining to the internal metabolite w by $\pi_w^{\mathrm{de/in}} = d \cdot |G_w^{-/+}|$, whereby $G_w^{-/+}$ denote the lower and upper boundary, respectively, of the validity range $[G_w^-, G_w^+]$ of the dual variable corresponding to metabolite w, which is provided by the LP solver (we choose $d = 0.2$). In case the provided validity boundaries deviate less than $1e^{-5}$ from b_w, which is an indicator of a degenerate problem with respect to our model setup and utilized solver, we use $G_w^{-/+} = b_w \mp 5e^{-4}$. We apply the same boundaries if the validity ranges indicate a negative range which is clearly non-informative. In case validity ranges take values $\pm\infty$, we limit them to a value of $\pm 1e^4$.

All shadow prices were normalized such that optimization of each objective yields values ranging between zero and one to enable a reasonable comparison. An outcome of one indicates the optimum, which in the case of minimizing total flux is the minimum flux.

4.5. Representative Pareto front solutions adjacent to ^{13}C flux measurements

We identify the elements of the representative Pareto front that are closest to the measured flux phenotypes. To this end, we determine flux distributions $\bar{\mathbf{f}}^{\exp}$ in the solution space Γ with minimum Euclidean distance to the experimental flux distributions. The computation is formulated as a quadratic optimization problem

$$\bar{\mathbf{f}}^{\exp} = \mathrm{argmin}_{\mathbf{f}\in\Gamma} \sum_i \frac{(f_i - f_i^{\exp})^2}{\sigma_i^{\exp}}, \tag{5}$$

whereby $f_i^{\exp}$ denotes the experimentally determined flux through reaction i and $\sigma_i^{\exp}$ the associated measurement error, which is used to weight the individual contributions. The summation is executed only for the reactions with measured flux values. The obtained flux distributions $\bar{\mathbf{f}}^{\exp}$ are fully determined, which is tested by fixing the value of the objective function of Eq. (5) and minimizing the Euclidean norm of $\bar{\mathbf{f}}^{\exp}$. The flux distributions with lowest distance to the Pareto front with respect to the considered experiments are then calculated as

$$\bar{\mathbf{f}} = \mathrm{argmin}_{\mathbf{f}\in\Gamma^*} \sqrt{\sum_p (z_p(\mathbf{f}) - z_p(\bar{\mathbf{f}}^{\exp}))^2}. \tag{6}$$

Here, Γ^* denotes the representative Pareto front and $z_p(\mathbf{f})$ the value of objective function p for the flux distribution $\mathbf{f}$. The fluxes are normalized in advance such that the values of the individual objective functions range between zero and one, to equally weight the three dimensions.

4.6. Metabolic network model

We examine a model of central carbon metabolism of *E. coli* published by Schuetz et al. (2007). The model comprises 74 unique reactions (given in Table S1), whereof 14 are transporters, and 61 metabolites (given in Table S2), whereof 47 metabolites are internal and, therefore, their concentrations have to obey the steady-state assumption. The metabolic network is able to import acetate, ethanol, glucose, nitrate and oxygen and to export acetate, ATP, biomass, carbon dioxide, ethanol, formate, lactate, nitrite, pyruvate and sucrose. Import of acetate and ethanol is disabled in the examined settings. Since ADP is an external metabolite in this model, the export of ATP does account for ATP regeneration rather than ATP *de novo* synthesis. The biomass export reaction comprises all metabolites from central carbon metabolism in appropriate ratios to support growth. The sum of glucose import by the reactions *mglABC* and *ptsGHI* is constrained from above arbitrarily by one. Isozymes in the model were deleted. In accordance with the utilized experimental data, nitrate import is deactivated. The utilized objective functions with respect to maximum ATP and biomass yield are *maint* and *biomass*, respectively.

4.7. Software

We use lpsolveAPI in the R environment for solving the linear programs and for the statistical analysis as well as Tomlab in the Matlab environment for solving the quadratic optimization problems.

Author's contributions

MSH and ZN designed and conceived the study. MSH carried out the computational analysis. MSH and ZN wrote the manuscript. All authors read and approved the final manuscript.

Acknowledgements

MSH and ZN would like to acknowledge the financial support of PROMICS, a Research Unit 1186 of the German Research Foundation.

Appendix A. Supplementary data

Supplementary data associated with this article can be found, in the online version, at http://dx.doi.org/10.1016/j.biosystems.2016.04.005.

References

Bazaraa, M.S., Jarvis, J.J., Sherali, H.D., 2010. Linear Programming and Network Flows. John Wiley & Sons, Inc.
Chubukov, V., Gerosa, L., Kochanowski, K., Sauer, U., 2014. Coordination of microbial metabolism. Nat. Rev. Microbiol. 12 (5), 327–340.
Desvergne, B., Michalik, L., Wahli, W., 2006. Transcriptional regulation of metabolism. Physiol. Rev. 86, 465–514.
Edwards, J.S., Ibarra, R.U., Palsson, B.Ø., 2001. *Insilico* predictions of *Escherichiacoli* metabolic capabilities are consistent with experimental data. Nat. Biotechnol. 19 (2), 125–130.
Edwards, J.S., Palsson, B.Ø., 2000. The *Escherichiacoli* MG1655 in silico metabolic genotype: its definition, characteristics, and capabilities. Proc. Natl. Acad. Sci. U. S. A. 97 (10), 5528–5532.
Fell, D., 2005. Enzymes, metabolites and fluxes. J. Exp. Bot. 56 (410), 267–272.
Gerosa, L., Sauer, U., 2011. Regulation and control of metabolic fluxes in microbes. Curr. Opin. Biotechnol. 22 (4), 566–575.
Helm, M., 2006. Post-transcriptional nucleotide modification and alternative folding of RNA. Nucleic Acids Res. 34 (2), 721–733.

Ho, J.K., 2000. Computing true shadow prices in linear programming. Informatica 11 (4), 421–434.
Ibarra, R.U., Edwards, J.S., Palsson, B.Ø., 2002. *Escherichiacoli* K-12 undergoes adaptive evolution to achieve *insilico* predicted optimal growth. Nature 420, 186–189.
Kitano, H., 2007. Towards a theory of biological robustness. Mol. Syst. Biol. 3, 137.
McCarl, B.A., Rister, M.E., Stokes, J.R., 1996. Improving shadow price information: obtaining relevant shadow prices from problems with decomposable objectives. Am. J. Agric. Econ. 78, 699–705.
Miettinen, K., 1999. Nonlinear Multiobjective Optimization. Kluwer Academic Publishers.
Motlagh, H.N., Wrabl, J.O., Li, J., Hilser, V.J., 2014. The ensemble nature of allostery. Nature 508 (7496), 331–339.
Orth, J.D., Thiele, I., Palsson, B.Ø., 2010. What is flux balance analysis? Nat. Biotechnol. 28 (3), 245–248.
Reznik, E., Mehta, P., Segrè, D., 2013. Flux imbalance analysis and the sensitivity of cellular growth to changes in metabolite pools. PLoS Comput. Biol. 9 (8), e1003195.
Salgado, H., Peralta-Gil, M., Gama-Castro, S., Santos-Zavaleta, A., Mu niz-Rascado, L., García-Sotelo, J.S., Weiss, V., Solano-Lira, H., Martínez-Flores, I., Medina-Rivera, A., Salgado-Osorio, G., Alquicira-Hernández, S., Alquicira-Hernández, K., López-Fuentes, A., Porrón-Sotelo, L., Huerta, A.M., Bonavides-Martínez, C., Balderas-Martínez, Y.I., Pannier, L., Olvera, M., Labastida, A., Jiménez-Jacinto, V., Vega-Alvarado, L., del Moral-Chávez, V., Hernández-Alvarez, A., Morett, E., Collado-Vides, J., 2013. RegulonDB v8.0: omics data sets, evolutionary conservation, regulatory phrases, cross-validated gold standards and more. Nucleic Acids Res. 41, D203–D213.
Savinell, J., Palsson, B.Ø., 1992. Network analysis of intermediary metabolism using linear optimization. I. Development of mathematical formalism. J. Theor. Biol., 421–454.
Savinell, J.M., Palsson, B.Ø., Arbor, A., 1992. Network analysis of intermediary metabolism using linear optimization. II. Interpretation of hybridoma cell metabolism the uses of linear optimization theory to calculate and interpret fluxes in metabolic. J. Theor. Biol., 455–473.
Schuetz, R., Kuepfer, L., Sauer, U., 2007. Systematic evaluation of objective functions for predicting intracellular fluxes in *Escherichia coli*. Mol. Syst. Biol. 3, 119.
Schuetz, R., Zamboni, N., Zampieri, M., Heinemann, M., Sauer, U., 2012. Multidimensional optimality of microbial metabolism. Science 336 (4), 601–604.
Strum, J.E., 1969. Note on “Two-Sided Shadow Prices”. J. Acc. Res. 7 (1), 160–162.
Varma, A., Palsson, B.Ø., 1994. Metabolic flux balancing: basic concepts, scientific and practical use. Nat. Biotechnol. 12 (10), 994–998.